Correction of I-123 MIBG uptake with multi-window methods for standardization of the heart to mediastinum ratio

Correction of I-123 MIBG uptake with multi-window methods for standardization of the heart to mediastinum ratio

Kenichi Nakajima [a], Kosuke Matsubara [b], Takehiro Ishikawa [c], Nobutoku Motomura [d], Ryo Maeda [c], Nasima Akhter [a], Koichi Okuda [a], Junichi Taki [a] and Seigo Kinuya [a]

a. Department of Biotracer Medicine, Kanazawa University Graduate School of Medical Sciences, Kanazawa, Japan
b. Department of Radiological Technology, Kanazawa University Hospital, Kanazawa, Japan
c. FUJIFILM RI Pharma, Co, Ltd., Tokyo, Japan
d. Toshiba Medical Systems, Co, Ltd., Tochigi, Japan
Correspondence
Kenichi Nakajima, MD
Department of Biotracer Medicine, Kanazawa University Graduate School of Medical Science, 13-1 Takara-machi, Kanazawa, 920-8641, JAPAN
Tel +81-76-265 –2333, Fax +81-76 234 -4257
E-mail: nakajima@med.kanazawa-u.ac.jp
Short title: ^{123}I MIBG uptake and multi-window correction

J Nucl Cardiol 2007;14:843-51
http://www.onlinejnc.com/article/PIIS1071358107005478/abstract

ABSTRACT

Background: To overcome differences in a collimator choice for a ^{123}I-MIBG heart to mediastinum (H/M) ratio, we examined multi-window correction methods with ^{123}I-dual-window (IDW) and triple-energy-window (TEW) acquisition.

Methods and Results: Standard phantoms which consisted of heart, mediastinum, lung and liver, were generated. Three correction methods were compared: TEW and two IDW methods (IDW_0 and IDW_1). Low-energy high-resolution (LEHR), medium-energy (ME) and ^{123}I specific low-medium-energy high-resolution (LMEHR) collimators were used. Clinical studies were performed in 10 patients. In the phantom study, the H/M ratio was significantly underestimated without correction both with the LEHR and ME collimators (70% and 88% of the true value). When H/M with the LEHR collimator was divided by uncorrected H/M with the ME collimator, the ratio was 80%+/-4%, 98%+/-5%, 104%+/-7%, 98%+/-5% for no correction, TEW, IDW_0 and IDW_1 methods, respectively. Clinical studies with the LEHR collimator after TEW

(uncorrected average H/M ratio 1.86+/-0.23, corrected 2.47+/-0.46) and IDW (2.46+/-0.46) correction provided comparable values to the uncorrected ME collimator (2.56+/-0.46).

Conclusions: The H/M ratio with the ME collimator after application of the TEW or IDW methods was the most accurate method in the phantom study. However, the corrected H/M ratios with the LEHR collimator provided comparable H/M ratios to the uncorrected ME data in phantom and clinical studies.

Key words
^{123}I meta-iodobenzylguanidine, collimator, iodine-dual-energy window method, triple-energy window method, quantification

Iodine-123 (^{123}I) labeled meta-iodobenzylguanidine (MIBG) is becoming an important and attractive tool for cardiac radionuclide imaging because of its characteristic markers in terms of its autonomic cardiac activity. [1-3] ^{123}I-MIBG was first approved by the Japanese Health and Welfare Ministry in 1992, and has been accepted for clinical routine use. [2] Based on clinical evidence, Japanese Circulation Society guidelines for nuclear cardiology listed use of MIBG as Class I (general agreement of effectiveness and usefulness) and Class IIa (conflicting evidence but in favor of usefulness/efficacy) or IIa' (conflicting evidence but in favor of usefulness/efficacy in Japan) for the evaluation of severity, prognosis, therapeutic effect, vasospastic angina and diabetic neuropathy. [4] However, there has been a discussion about the lack of standards for acquisition and processing, resulting in institute-specific procedure and standards. [5, 6] Although heart to mediastinum (H/M) ratios in a planar study have been used for practical quantification method, to date, no large-scale investigation has been conducted because of these lack of standards.

Normal values and within-subject variability of MIBG distribution of the heart have also been studied. [1, 3, 7, 8] Among factors influencing the inter-institute variability, collimator choice was one of the most important issues to be overcome, because Compton scatter and septal penetration from high-energy 529 keV photons (1.4%) overlapped onto the 159 keV (83%) main window, and caused image degradation and inaccuracy of ^{123}I quantification. Therefore, investigators have recommended the use of a medium-energy collimator, a specific deconvolution technique adapted for ^{123}I and multiple-window method. [9-13] Among these proposals, we focused on the multiple-window method in this study as a practical approach to be performed in any institute, not influenced by camera venders and collimators.

We hypothesized that

improvement in quantification can be achieved by a multiple-window approach. Preparation of the phantom should be simple and reproducible for measuring the H/M ratio. Since the H/M ratio can be calculated mathematically in the standard phantom, the accuracy of the method was easily confirmed in various types of data acquisition systems. Finally, this method was applied to a patient study and the validity was compared with the precedent phantom and clinical studies.

METHODS

Preparation of phantoms

We have preliminary performed block-model phantom studies for generating standardization phantom.[14] The block models consisted of rectangular bottles, and acrylic plates (9.7mm/plate) were made. Each block size was 58x58x90 mm or 84x35x90 mm, and 15 to 18 blocks and 3 acrylic plates were combined to make various attenuation and scatter conditions. Since nearly identical theoretical values could be obtained from the block-model study, we were able to make more realistic phantom configurations of the heart, mediastinum and liver in this study. The structure of the phantom is shown in Figure 1. This phantom was designed for measuring the planar H/M ratio, and was not for calculating three-dimensional distribution as in the SPECT study. Since the purpose of this study was to standardize the H/M ratio among different collimator types and manufacturers by eliminating septal penetration and/or scatter, we tried to simplify the structure as far as possible, so that the same H/M ratio was always calculated in any institutes. Each organ part was designed so that the radioactivity was uniform in the organ region of interest (ROI). The size of the phantom was 380 mm in width and length, and the thickness of the each organ was flat and constant. The thickness of each organ part was adjusted by changing the number of slices. Four types of acrylic slice parts, with a thickness of 5mm per slice, were combined and arranged into various numbers and orders. The upper and lower slice was 10 mm in thickness. Since all the organ parts were connected as one compartment, no adjustment of radionuclide concentration for each organ part was required. A total of 8 H/M ratios could be calculated with anterior and posterior views from the four phantoms (Table 1). In the phantom studies, true H/M ratios were mathematically calculated in these models assuming the linear attenuation coefficient (μ) of ^{123}I for water as 0.147/cm. The standard equation for attenuation, that is, $e^{-\mu \cdot x}$, where x was thickness of attenuation, was used. A slice was divided into 0.05mm of thin slices and the summation of count was calculated using Mathematica software (version 5.2, Wolfram Research, Inc, Champaign, IL, US). The phantom measurement was repeated with and without three acrylic plates (9.7mm/plate) over the phantom as scatter media.

Data acquisition and correction methods

Planar images were simultaneously obtained with five energy windows, and were combined to make three correction methods: that is, windows 1 to 5 were 132-142, 143-175, 176-186, 187-208 and 209-294 keV. The triple-energy window (TEW) method used the main I-123 window (143-175 keV) and upper (176-186 keV) and lower (132-142 keV) subwindows. [15] The width of the upper and lower window was 7% of the main peak, which was wider than the original 3% scatter rejection windows. The ^{123}I-dual-window (IDW) method used an energy window on the high-energy side to estimate the number of scattered 529 keV photons, in which an original upper window (176-208 keV, IDW_0) by Motomura et al. [12] and a wide upper window (176-294 keV, IDW_1) were examined. When the count in windows 1 to 5 was defined as C_1 to C_5, and the width (keV) as W_1 to W_5, then the following resulted:

Corrected count by TEW method = $C_2 - (C_1/W_1+C_3/W_3) \cdot W_2/2$

Corrected count by IDW_0 method = $C_2 - (C_3+C_4) \cdot (W_2/ (W_3+W_4))$

Corrected count by IDW_1 method = $C_2 - (C_3+C_4+C_5) \cdot (W_2/(W_3+W_4+W_5))$.

The energy window setting was explained in Figure 2. More intuitively, the TEW method subtracted mainly scattered counts by trapezoid approximation from the main W2 window count, whereas the IDW method subtracted mainly septal penetration counts by rectangular approximation. The original TEW and IDW methods used Butterworth filtering for subwindow images and subtracted the filtered image from the main-window image. However, in this study no image subtraction was performed to avoid a decrease in count and an increase in noise even after filtering. Subwindow images were used only for calculating the counts on the same ROIs as the main window.

Collimators

Low-energy high resolution (LEHR) and medium-energy (ME) collimators were used for both phantom and clinical studies. A low-medium-energy high-resolution (LMEHR) collimator specifically designed for ^{123}I high-energy photons was also used for the phantom study. The resolution was 7.4, 10.1 and 7.6 mm for LEHR, ME and LMEHR collimators at a collimator-to-source distance of 10 cm, respectively. The sensitivity of the collimators was 5.5, 6.1 and 5.4 cpm/kBq, respectively.

Clinical studies

Ten consecutive patients indicated for MIBG study were examined. ^{123}I-MIBG (111 MBq) was injected intravenously, and the planar and SPECT images were obtained with Toshiba GCA-9300A three-detector gammacameras and LEHR collimators. For this study, anterior images were obtained 3 hours after injection with both LEHR and ME collimators using 256 x 256 matrices for 2 minutes.

Data processing for H/M ratio

The ROIs were set over the

heart and the upper one-third of the mediastinum on the main-window image. The same ROIs were used to measure the count on the 5 subwindow images. The H/M ratios were calculated by average heart count divided by average mediastinal count.

Statistics

Average counts in ROIs were used for image data analysis. Statistics of the average and standard deviation (SD) were calculated. An analysis of variance for the mean was performed based on groups with collimator types and correction methods. A paired t test was also used for the comparison of correction methods. A linear regression line for two variables was calculated by standard linear regression analysis. A p value <0.05 was considered significant.

RESULTS

Phantom study

When H/M ratios were calculated with the 4 types of phantoms in the anterior and posterior views with and without 3 scatter plates, a total of 16 data points were obtained. Table 2 shows the calculated H/M ratios divided by the mathematically calculated true H/M ratios using LEHR, ME and LMEHR collimators. The uncorrected H/M ratio with a LEHR collimator was 0.71 +/- 0.08 and 0.70 +/- 0.08 with and without three scatter plates, respectively. The TEW and IDW_0 methods showed the ratio of 0.86 +/- 0.04 and 0.91 +/- 0.06 without acrylic plates, which still underestimated the true values. On the other hand, results from ME collimator demonstrated 0.88 +/- 0.06 without correction, and 1.02 +/- 0.02, 0.99 +/- 0.05 and 0.96 +/- 0.05 with TEW, IDW_0 and IDW_1 correction methods, respectively. The results from a LMEHR collimator showed a similar tendency as that of a ME collimator. Therefore, the H/M ratios with a ME collimator plus TEW or IDW_0 correction methods ranged from 0.97 to 1.05 which was near the theoretical value of 1. When the H/M ratio with a LEHR collimator was divided by the uncorrected H/M ratio with a ME collimator, the TEW, IDW_0 and IDW_1 correction methods showed an average of 0.98, 1.04 and 0.98 without scatter plates, and 1.00, 1.03 and 1.00 with scatter plates. This indicated that the scatter correction by TEW and IDW method showed comparable values with uncorrected H/M ratio with ME collimators.

The relationship between the uncorrected H/M ratio with ME collimator and H/M ratios with LEHR collimator is shown in Figure 3. The uncorrected H/M ratio with LEHR collimator (y) was significantly underestimated, but it showed linear relationship with the H/M with ME collimator (x), $y=0.68x + 0.28$, $r^2=0.994$ (n=16). After correction by the TEW, IDW_0 or IDW_1 methods, three regression lines were nearly similar on the line of identity.

Uncorrected H/M ratios with ME and LMEHR collimators revealed an excellent correlation of $r^2=0.997$ and

0.993 with and without scatter plates (Figure 4).

Clinical studies

Images of five windows from case No. 7 are shown in Figure 5. Although the maximum count in the main-window image was similar in this case, scatter and septal penetration from the ^{123}I high energy was significantly higher by the LEHR collimator. The image contrast with the ME collimator was significantly higher than that with the LEHR collimator. Table 3 showed the results of all clinical studies. Without correction methods, the H/M ratio with LEHR was 1.86 +/- 0.23 and that with the ME collimator was 2.56 +/- 0.46 ($p<0.0001$). When TEW or IDW_0 correction was applied to the LEHR data, the H/M ratio increased to 2.47 +/- 0.46 and 2.46 +/- 0.46, respectively. Based on a paired t test, the H/M ratios between TEW and IDW_0 methods showed no significant difference, while the H/M ratios by IDW_1 were significantly lower than those from TEW and IDW_0 methods ($p=0.0035$ and $p=0.0063$). Similarly to the phantom data, the H/M ratios with and without correction were divided by uncorrected ME data. The ratio was underestimated to 0.73 +/- 0.06 without correction, but the ratio was improved to 0.96 +/- 0.05, 0.96 +/- 0.05 and 0.88 +/- 0.06 with the TEW, IDW_0 and IDW_1 correction methods. When the relationship of the H/M ratio between the ME collimator (X) and LEHR collimator (Y) was examined, a linear correlation was observed: $Y = 0.45X + 0.70$ ($R^2 = 0.80$) (Figure 6, regression line B). After correction by IDW_0 methods, the linear regression line became $Y=0.95 X + 0.033$ ($R^2 = 0.91$) (regression line C).

DISCUSSION

The main conclusion of this study was that the H/M ratio without correction of septal penetration and scatter underestimated the true H/M ratio, and the multi-window correction improved the H/M values. Based on the phantom study, H/M ratios with a ME collimator plus TEW or IDW_0 correction methods were nearly equal in value to the theoretical H/M ratio. However, application of TEW or IDW correction methods could provide comparable values to the uncorrected data from the ME collimator. Thus, for practical purposes, the multi-window correction method may be used for comparing data with ME collimators.

Structure of the phantom

The phantom structure in this study was designed specifically to evaluate planar MIBG H/M ratio. Therefore realistic three-dimensional distribution as reconstructed from SPECT study was not sought after. The morphologically realistic phantom that consisted of lung, mediastinum, heart and vertebra with different amount of radioisotope concentration and appropriate attenuation media is certainly useful for evaluating quantitative SPECT studies. However, reproducibility of phantom concentration in each organ part was not always good,

resulting in technical fluctuation of measured H/M ratios. Since the aim of this study was to standardize the planar H/M ratio among different collimator types and manufacturers by eliminating septal penetration and scatter, we simplified the structure as far as possible, so that the calculated H/M ratio was identical in any institutes. Conversely, we found difficulties in standardization by using conventional phantom as a RH2 phantom (Kyoto Kagaku, Japan) and an anthropomorphic phantom (Data Spectrum, Hillsborough, NC, USA).

Moreover, the high-energy (529 keV) photon caused significant amount of septal penetration, and the high background activity was the results of multiple complex scatters. The septal penetration and/or scatter distribution eventually showed broad distribution all over the field of view, which was also shown in the images of 187-209 and 210-294 keV windows in Figure 5. The distribution of septal penetration did not seem to reflect the precise structure of tracer distribution both in the phantom and clinical studies. The idea of IDW method aimed at eliminating this septal penetration from the high-energy photons. In contrast, the scatter image in the window just below the ^{123}I main window (132-142keV) showed somewhat similar distribution to the main window in Figure 5. The idea of TEW method aimed at eliminating mainly scatter fraction as well as septal penetration.

The mediastinal ^{123}I concentration was actually low and distributed in the large thickness than the heart activity. Thus the mediastinal concentration was in fact lower than the clinical H/M ratio of 2-3:1, which was also confirmed by the anthropomorphic torso phantom study[16]. However, in our phantom study, actual tracer distribution was relatively thin but was covered with thick acrylic scatter media. The thickness was adjusted to obtain optimal range of H/M ratios as seen in clinical studies. This sort of simplification has also been used in Nuclear Medicine studies for thyroid phantom or liver phantoms with defects in the past. Finally, good correlation with more complicated phantom shapes [9, 13] and acceptable agreement with clinical studies support adequacy of this phantom for the practical purpose of standardizing planar H/M ratio.

Effect of collimator choice

The effect of collimator choice substantially influenced estimation of H/M ratios. Inoue et al. studied the collimator selection for a ^{123}I planar study and found that use of an ME collimator provided high quantitative accuracy and may enhance reliability in the evaluation. [9] The same group also investigated the use of a special LEHR collimator in addition to LEHR and ME collimators. [10] For SPECT the ME collimator was comparable or superior to the LEHR collimator, but depended on the condition of the MIBG defect, cavity/myocardial ratio and lung activity. Verberne et al. have studied phantom experiments using various activities in the heart, lung and liver. [11] Planar H/M ratios were influenced by scatter and septal

penetration from increasing amounts of liver activity, and the effects were less pronounced for ME collimators. Despite these studies in favor of the ME collimator, most institutes have used LEHR collimators, partly because the exchange of ME and LEHR collimators among ^{99m}Tc studies are a burden for demanding clinical settings, and medical staff feel that the SPECT image quality of LEHR is acceptable for visual analysis. Thus, practical correction methods of the planar H/M ratio by using LEHR collimator should be sought after, even if SPECT studies were still performed by LEHR collimator.

Multi-window methods

Multi-window methods, including triple- and dual-energy window methods, and a deconvolution method for septal penetration compensation (DSP) have been proposed. An iterative reconstruction with DSP was reported to yield more accurate heart-to-calibration ratios. [16, 17] On the other hand, multi-window methods could be easily applied by any institution, considering the capability of current camera-computer systems. However, their use has not been well-validated and they lack clinical experience. The TEW method was known to increase the H/M ratio, but it reduced heart count density and might have caused uncertainty in defect contrast. [11] The narrow subwindows on both sides of the main window caused instability and noise from the viewpoints of image quality. The dual-window method was proposed and examined for the feasibility of methods by phantom studies, but has not been validated with respect to its accuracy and clinical usefulness. [12, 13] The original TEW and IDW methods required filtering of subwindow images to reduce high-frequency noises and subtracted the filtered image from the main window image. Since this process reduces image count and the quality depends on the filter types, we decided to use the subwindow images only for calculation of counts in ROIs. The SPECT imaging could thus be performed by conventional methods with sufficient counting statistics.

Both TEW and IDW methods provided comparable H/M values with respect to scatter and septal penetration correction. However considering the relatively narrow subwindows on both sides of the main window, the value may be susceptible to statistical noise. [11] Although we found comparable results in IDW_0 and IDW_1, the IDW_1 method seemed to show a slightly lower H/M ratio (0.84-0.94) than IDW_0 (0.88-0.99) with reference to the theoretical values. Although we assumed the IDW_0 method was appropriate, additional studies are required in clinical settings to confirm this.

Comparison with reported data

Our results are comparable with the previously published data, although the setting of the phantom was not identical. In the Kanto district in Japan, phantom studies using heart-liver phantom RH2 (Kyoto Kagaku, Kyoto, Japan), which has also been used by other

investigators, have been conducted. [12, 13] The compartments of the heart, liver, lung and mediastinum were filled with ^{123}I MIBG with a radioactivity ratio of 15:10:8:1 (personal communication from Junichi Yamazaki, MD and Shohei Yamashina, MD). The main window was set to 143-175 keV, and the upper subwindow was set to 176-294 keV, which was the same setting as the IDW_1 method. The same phantom experiments were performed in eight institutions, including Shimadzu/Picker IRIX, GE Starcam, Toshiba GCA 7200 and GCA 9300, Shimadzu PRISM 2000 and PRISM 3000, SNC510R. The results of the H/M ratios measured by ME and LEHR collimators are plotted in Figure 6. We found that the results were in line with our standard phantom experiments, although a slight variation was observed due to possible differences in preparation of the radioisotope concentration and camera systems. According to a MIBG examination questionnaire survey of heart failure conducted in Japan involving109 institutions, various normal values were used in each hospital. [18] The averages of the normal values were 2.25+/- 0.27 and 2.78+/-0.32 for the LEHR and ME collimators in the early images, and 2.36+/-0.24 and 3.17+/- 0.29 for the delayed images, respectively. The values were again in line with those of the linear regression line shown in Figure 6 (line A). The clinical H/M ratios in this study are plotted in Figure 6 for comparison. The relationship of the H/M ratios between ME and LEHR collimators showed a slightly lower slope in the clinical study than those in the phantom study, probably reflecting the difference in MIBG distribution and scatter patterns. We could note that the corrected H/M values were approximately on the line of identity.

When published MIBG studies were observed, two groups of H/M normal values were reported, although the precise collimator information was not available from all studies. In a group, the delayed H/M ratio ranged from 2.1 to 2.4 [7, 19-23] On the other hand, another group showed higher delayed H/M ratio from 2.8 to 3.0. [24-26] In the latter group, two studies used the LEGP collimator that covers the high-energy photons for ^{123}I, and one seemed to use a low-energy collimator with TEW correction. The collimator design for ^{123}I as used by Inoue et al. and for the LMEHR collimator as in our study provides higher H/M values as is also the case with the ME collimator. [10] The differences in average values reflected the difference in two types of collimator designs; that is, for low energy suitable for ^{99m}Tc and for covering ^{123}I high energy including some LEGP collimators of Japanese manufacturers and the ME collimator.

Standardization of MIBG parameters

Although many independent studies have demonstrated the usefulness of MIBG studies for ischemic heart diseases and these are accepted as a part of the Japanese nuclear cardiology guidelines, [4] the same standard of acquisition and processing could not be extended to other institutions, which also

hampered the multi-center investigation. Therefore, large-scale evidence has been lacking for the wider use of a MIBG study. Although some studies have recommended the use of ME collimators, many hospitals still continue to use low-energy collimators, and most of the precedent data have been accumulated with low-energy collimators. Therefore, the relationship among those studies should be clarified. In the present study, we generated a simple phantom with one compartment filled with fluid of the same concentration. Previous phantom studies required filling of the separated organ compartments with different radionuclide concentrations, which resulted in the variation of the H/M ratio even if the ^{123}I concentration was carefully prepared. In contrast, our phantoms had constant thickness for each organ but yielded comparable values with the more complicated chest-heart phantom. The preference of the camera and collimator types would differ in future studies, so that simple phantoms like this will help to calibrate inter-institutional differences in the H/M ratio. Another factor for variation is location of ROIs of the heart and mediastinum. Automatic selection would improve the reproducibility among institutions.

Conclusion

Aiming at the standardization of a ^{123}I-MIBG uptake with H/M ratios, we generated standard phantom consisting of heart, lung and liver having the same radionuclide concentration. The H/M ratio was significantly underestimated without correction in both the phantom and clinical studies. However, after triple-energy or iodine-dual-window corrections, the underestimation was significantly improved. The use of either TEW or IDW_0 corrections with a ME collimator was the most accurate compared with the theoretical values in the phantom study. The application of IDW or TEW correction methods with a LEHR collimator yielded comparable values with the use of a ME collimator.

Acknowledgement

We thank Minoru Tobisaka, RT, and Shigeto Matsuyama for technical assistance with the clinical studies. This study was supported by a Grant-in-Aid for Scientific Research (C) in Japan.

References

1. Hattori N, Schwaiger M. Metaiodobenzylguanidine scintigraphy of the heart: what have we learnt clinically? Eur J Nucl Med 2000;27:1-6.
2. Yamashina S, Yamazaki J. Neuronal imaging using SPECT. Eur J Nucl Med Mol Imaging 2007; 34:S62-73
3. Momose M, Tyndale-Hines L, Bengel FM, Schwaiger M. How heterogeneous is the cardiac autonomic innervation? Basic Res Cardiol 2001;96:539-46.
4. Tamaki N, Kusakabe K, Kubo A, Kumasaki T, Shimamoto K, Senda S, et al. Guidelines for Clinical Use of Cardiac Nuclear Medicine (JCS 2005). Circulation Journal 2005;69 Suppl. IV:1125-202.
5. Yamashina S, Yamazaki J. Role of MIBG myocardial scintigraphy in the assessment of heart failure: the need to establish evidence. Eur J Nucl Med Mol Imaging 2004;31:1353-5.
6. Motherwell DW, Petrie MC, Martin W, Cobbe SM. ^{123}I-Metaiodobenzylguanidine in chronic heart failure: Is there a clinical use? Nucl Med Commun 2006;27:927-31.
7. Nakajima K, Taki J, Tonami N, Hisada K. Decreased ^{123}I-MIBG uptake and increased clearance in various cardiac diseases. Nucl Med Commun 1994;15:317-23.
8. Somsen GA, Verberne HJ, Fleury E, Righetti A. Normal values and within-subject variability of cardiac I-123 MIBG scintigraphy in healthy individuals: implications for clinical studies. J Nucl Cardiol 2004;11:126-33.
9. Inoue Y, Suzuki A, Shirouzu I, Machida T, Yoshizawa Y, Akita F, et al. Effect of collimator choice on quantitative assessment of cardiac iodine 123 MIBG uptake. J Nucl Cardiol 2003;10:623-32.
10. Inoue Y, Shirouzu I, Machida T, Yoshizawa Y, Akita F, Minami M, et al. Collimator choice in cardiac SPECT with I-123-labeled tracers. J Nucl Cardiol 2004;11:433-9.
11. Verberne HJ, Feenstra C, de Jong WM, Somsen GA, van Eck-Smit BL, Busemann Sokole E. Influence of collimator choice and simulated clinical conditions on 123I-MIBG heart/mediastinum

ratios: a phantom study. Eur J Nucl Med Mol Imaging 2005;32:1100-7.

12. Motomura N, Ichihara T, Takayama T, Aoki S, Kubo H, Takeda K. Practical compensation method of downscattered component due to high energy photon in 123I imaging [Abstract in English]. Kaku Igaku (Jpn J Nucl Med) 1999;36:997-1005.
13. Kobayashi H, Momose M, Kanaya S, Kondo C, Kusakabe K, Mitsuhashi N. Scatter correction by two-window method standardizes cardiac I-123 MIBG uptake in various gamma camera systems. Ann Nucl Med 2003;17:309-13.
14. Nakajima K, Motomura N, Matsubara K, Ishikawa T, Maeda R, Taki J, et al. Quantification of I-123 MIBG uptake by triple-energy window and dual-window methods independent on collimator selection. [Abstract]. J Nucl Med 2006;47:257P-8P.
15. Ichihara T, Ogawa K, Motomura N, Kubo A, Hashimoto S. Compton scatter compensation using the triple-energy window method for single- and dual-isotope SPECT. J Nucl Med 1993;34:2216-21.
16. Chen J, Garcia EV, Galt JR, Folks RD, Carrio I. Improved quantification in ^{123}I cardiac SPECT imaging with deconvolution of septal penetration. Nucl Med Commun 2006;27:551-8.
17. Chen J, Garcia EV, Galt JR, Folks RD, Carrio I. Optimized acquisition and processing protocols for I-123 cardiac SPECT imaging. J Nucl Cardiol 2006;13:251-60.
18. Nishimura T. *Heart failure and cardiac sympathetic neuronal function [in Japanese]*. Tokyo: Medical View, 2002:148-55.
19. Richalet JP, Merlet P, Bourguignon M, Le-Trong JL, Keromes A, Rathat C, et al. MIBG scintigraphic assessment of cardiac adrenergic activity in response to altitude hypoxia. J Nucl Med 1990;31:34-7.
20. Sakata K, Shirotani M, Yoshida H, Kurata C. Cardiac sympathetic nervous system in early essential hypertension assessed by 123I-MIBG. J Nucl Med 1999;40:6-11.
21. Kuwahara T, Hamada M, Hiwada

K. Direct evidence of impaired cardiac sympathetic innervation in essential hypertensive patients with left ventricular hypertrophy. J Nucl Med 1998;39:1486-91.

22. Agostini D, Babatasi G, Manrique A, Saloux E, Grollier G, Potier JC, et al. Impairment of cardiac neuronal function in acute myocarditis: iodine-123-MIBG scintigraphy study. J Nucl Med 1998;39:1841-4.
23. Matsuo S, Nakamura Y, Tsutamoto T, Kinoshita M. Impairments of myocardial sympathetic activity may reflect the progression of myocardial damage or dysfunction in hypertrophic cardiomyopathy. J Nucl Cardiol 2002;9:407-12.
24. Otsuka N, Ohi M, Chin K, Kita H, Noguchi T, Hata T,et al. Assessment of cardiac sympathetic function with iodine-123-MIBG imaging in obstructive sleep apnea syndrome. J Nucl Med 1997;38:567-72.
25. Hattori N, Tamaki N, Hayashi T, Masuda I, Kudoh T, Tateno M, et al. Regional abnormality of iodine-123-MIBG in diabetic hearts. J Nucl Med 1996;37:1985-90.
26. Morozumi T, Kusuoka H, Fukuchi K, Tani A, Uehara T, Matsuda S, et al. Myocardial iodine-123-metaiodobenzylguanidine images and autonomic nerve activity in normal subjects. J Nucl Med 1997;38:49-52.

Table 1. Phantom types and mathematically calculated H/M ratios

	Ratio of thickness				Mathematically calculated H/M	
	Heart	Mediastinum	Lung	Liver	Anterior view	Posterior view
Type A	4	1	2	4	3.59	4.48
Type B	6	2	3	6	2.60	3.50
Type C	5	2	3	5	2.25	2.80
Type D	5	3	4	6	1.55	1.80

Table 2. Calculated H/M ratios from chest-heart standard phantom

		No correction		TEW		IDW_0		IDW_1	
		mean	sd	mean	sd	mean	sd	mean	sd
Divided by true H/M ratio (n=8)									
LEHR	S-	0.71	0.078	0.86	0.037	0.91	0.063	0.86	0.046
	S+	0.70	0.082	0.86	0.030	0.88	0.049	0.84	0.053
ME	S-	0.88	0.055	1.02	0.019	0.99	0.049	0.96	0.047
	S+	0.86	0.052	1.05	0.009	0.97	0.047	0.93	0.039
LMEHR	S-	0.85	0.061	1.00	0.015	0.98	0.042	0.94	0.044
	S+	0.82	0.056	1.02	0.052	0.95	0.036	0.91	0.033
Divided by uncorrected H/M with ME collimator (n=8)									
		No correction		TEW		IDW_0		IDW_1	
		mean	sd	mean	sd	mean	sd	mean	sd
LEHR	S-	0.80	0.045	0.98	0.049	1.04	0.069	0.98	0.049
	S+	0.81	0.050	1.00	0.034	1.03	0.036	1.00	0.034
P values									
LEHR vs ME data									
	S-	0.0002		<0.0001		0.0132		0.0007	
	S+	0.0004		<0.0001		0.0022		0.0017	
LEHR vs uncorrected ME data									
	S-	0.0002		ns		ns		ns	
	S+	0.0004		ns		ns		ns	

S-: without scatter plates over the phantom

S+: with three scatter plates over the phantom

Table 3. Clinical MIBG study and H/M ratio

A. H/M ratios

	LEHR collimator				ME collimator			
case	No correction	TEW	IDW_0	IDW_1	No correction	TEW	IDW_0	IDW_1
1	2.17	3.06	3.10	2.40	3.00	3.90	3.52	3.38
2	2.14	3.12	3.03	2.81	3.23	4.61	3.86	3.73
3	1.44	1.65	1.64	1.64	1.72	2.58	2.06	1.95
4	1.89	2.60	2.58	2.37	2.90	4.43	3.56	3.39
5	1.73	2.15	2.17	1.84	2.25	2.89	2.62	2.50
6	1.89	2.54	2.53	2.37	2.39	3.29	2.80	2.68
7	1.71	2.25	2.20	2.08	2.39	3.40	2.79	2.69
8	1.99	2.83	2.86	2.60	2.98	4.81	3.76	3.48
9	2.00	2.38	2.41	2.34	2.47	3.02	2.86	2.75
10	1.65	2.13	2.11	2.00	2.32	3.30	2.73	2.64
mean	1.86	2.47	2.46	2.24	2.56	3.62	3.06	2.92
sd	0.23	0.46	0.46	0.35	0.46	0.77	0.58	0.55
P value vs. no correction	-	0.0015	0.0017	0.0102	-	0.0015	0.0467	n. s.

B. Divided by uncorrected H/M ratio with ME collimator

	LEHR collimator			
Case	No correction	TEW	IDW_0	IDW_1
1	0.72	1.02	1.03	0.80
2	0.66	0.97	0.94	0.87
3	0.83	0.96	0.95	0.95
4	0.65	0.89	0.89	0.82
5	0.77	0.96	0.96	0.82
6	0.79	1.06	1.06	0.99
7	0.72	0.94	0.92	0.87
8	0.67	0.95	0.96	0.87
9	0.81	0.97	0.98	0.95
10	0.71	0.92	0.91	0.86
mean	0.73	0.96	0.96	0.88
sd	0.06	0.05	0.05	0.06
P value vs. no correction	-	<0.0001	<0.0001	<0.0001

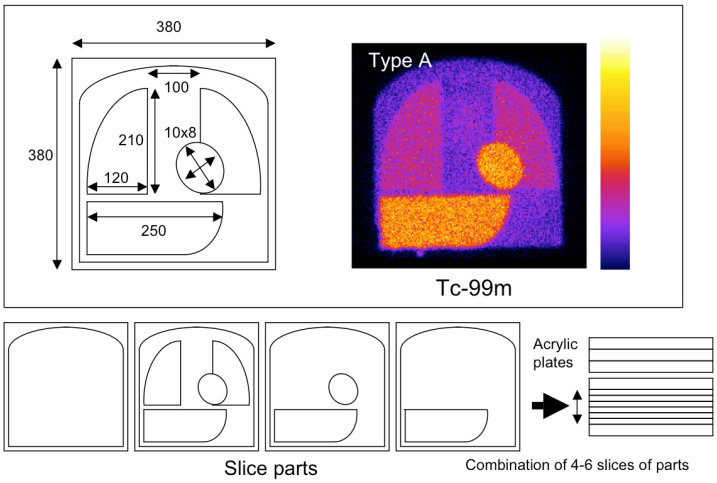

Figure 1

Structure of the phantom consisting of several combinations of plate types. The size of each compartment is shown in the left upper panel (unit: mm). The sample image was obtained by ^{99m}Tc (right upper panel). Organ parts consisted of several types of acrylic plates with a thickness of 5 mm.

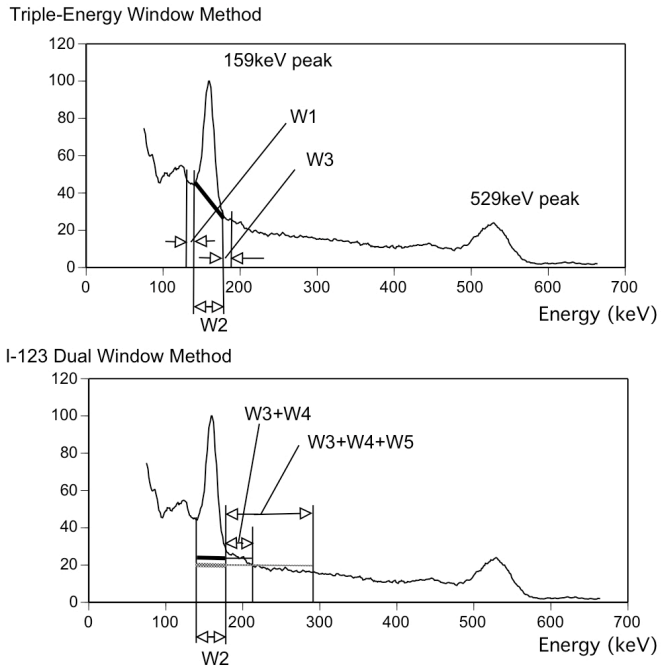

Figure 2

Schematic representation of TEW and IDW methods. Five energy windows (W1 to W5) are shown with the energy spectrum of ^{123}I obtained with LEHR collimator. The thick lines in the W2 window indicate subtracted counts.

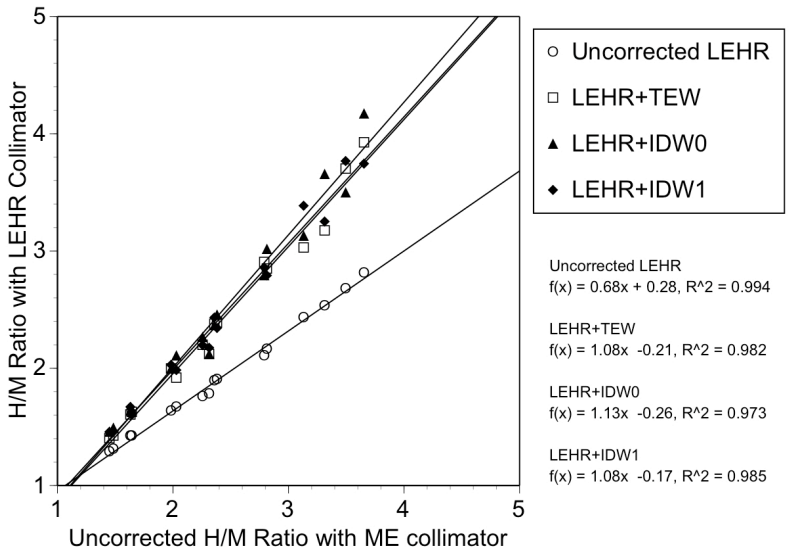

Figure 3

The relationship between the uncorrected H/M ratio with the ME collimator and the H/M ratios with the LEHR collimator.

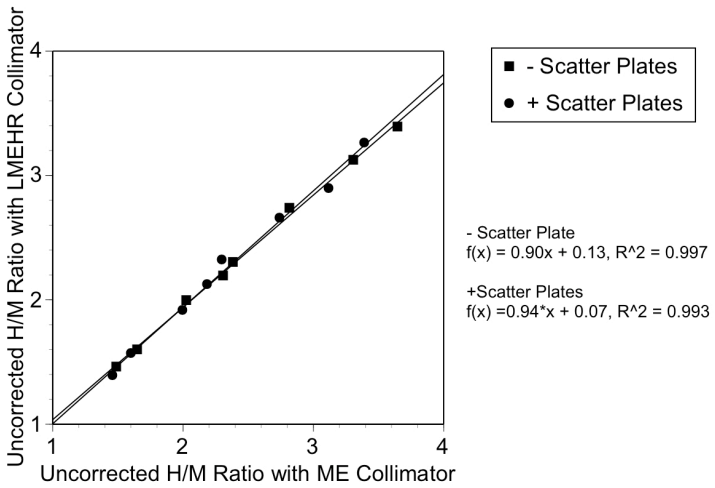

Figure 4

Correlation between uncorrected H/M ratios with the ME and LMEHR collimators.

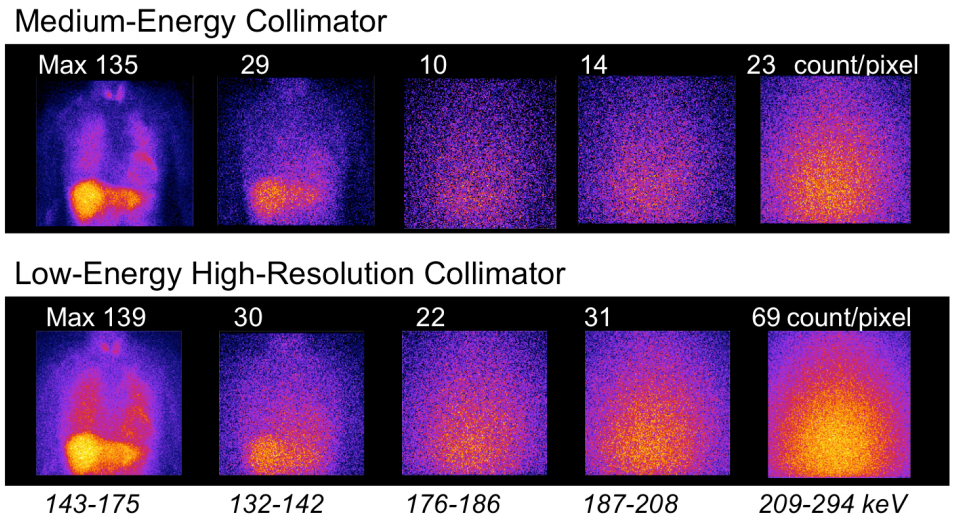

Figure 5

Images of 5 energy windows with the ME and LEHR collimators. Maximum count is shown on the image and normalized to 100% for each image. The left panel of the 143-175 keV image was obtained in the main window.

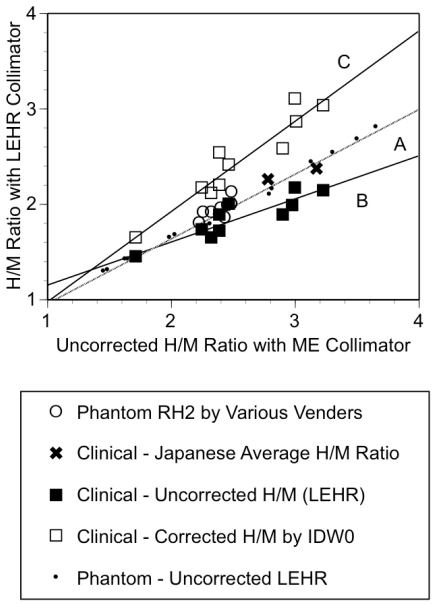

Figure 6

Relationship between the uncorrected H/M ratio with the ME collimator and with the LEHR collimator. Regression line A indicates this phantom study. Solid square and regression line B indicate the clinical MIBG study without correction. Open square and regression line C indicate clinical MIBG study after IDW_0 correction. Open circles are derived from RH2 phantom study from various venders. The two marks of x indicate average early and delayed H/M ratios in Japan.

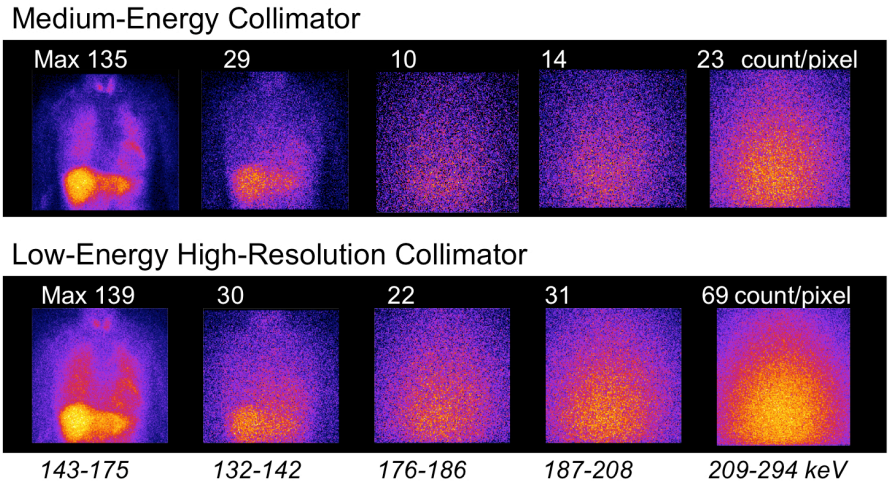
Medium-Energy Collimator
Max 135
29
10
14
23 count/pixel
Low-Energy High-Resolution Collimator
Max 139
30
22
31
69 count/pixel
143-175
132-142
176-186
187-208
209-294 keV